NeuroImage 140 (2016) 76–82

Contents lists available at ScienceDirect

NeuroImage

journal homepage: www.elsevier.com/locate/ynimg

# Different coupling modes mediate cortical cross-frequency interactions

Randolph F. Helfrich [a,b,*], Christoph S. Herrmann [c,d], Andreas K. Engel [a,1], Till R. Schneider [a,1]

[a] Department of Neurophysiology and Pathophysiology, University Medical Center Hamburg-Eppendorf, 20246 Hamburg, Germany
[b] Helen Wills Neuroscience Institute, University of California Berkeley, Berkeley, CA 94720, USA
[c] Experimental Psychology Lab, Center for excellence 'Hearing4all', European Medical School, University of Oldenburg, 26111 Oldenburg, Germany
[d] Research Center Neurosensory Science, University of Oldenburg, 26111 Oldenburg, Germany

ARTICLE INFO

*Article history:*
Accepted 13 November 2015
Available online 23 November 2015

*Keywords:*
Cross-frequency coupling
Phase-amplitude coupling
Oscillatory alpha–gamma interplay
Intrinsic coupling modes
Transcranial alternating current stimulation
Entrainment

ABSTRACT

Cross-frequency coupling (CFC) has been suggested to constitute a highly flexible mechanism for cortical information gating and processing, giving rise to conscious perception and various higher cognitive functions in humans. In particular, it might provide an elegant tool for information integration across several spatiotemporal scales within nested or coupled neuronal networks. However, it is currently unknown whether low-frequency (theta/alpha) or high-frequency gamma oscillations orchestrate cross-frequency interactions, raising the question of who is master and who is slave. While correlative evidence suggested that at least two distinct CFC modes exist, namely, phase-amplitude-coupling (PAC) and amplitude-envelope correlations (AEC), it is currently unknown whether they subserve distinct cortical functions. Novel non-invasive brain stimulation tools, such as transcranial alternating current stimulation (tACS), now provide the unique opportunity to selectively entrain the low- or high-frequency component and study subsequent effects on CFC. Here, we demonstrate the differential modulation of CFC during selective entrainment of alpha or gamma oscillations. Our results reveal that entrainment of the low-frequency component increased PAC, where gamma power became preferentially locked to the trough of the alpha oscillation, while gamma-band entrainment enhanced AECs and reduced alpha power. These results provide causal evidence for the functional role of coupled alpha and gamma oscillations for visual processing.



## Introduction

Cognition and conscious perception are thought to arise from neuronal interactions between functionally specialized but widely distributed cortical regions (Siegel et al., 2012). While phase synchronization between task-relevant cortical areas might integrate information across several spatial scales (Fries, 2005), cross-frequency coupling (CFC) has been suggested to constitute a flexible mechanism for information integration across temporal scales (Canolty and Knight, 2010). Hence, it might serve as a key mechanism for selective gating and processing of information within coupled or nested cortical networks and thus, subserve numerous cognitive functions in humans (Canolty and Knight, 2010; Engel et al., 2013; Voytek et al., 2010). However, the functional role of CFC is currently extensively under debate, given that (I) various methodological constrains hamper its interpretation (Aru et al., 2014), (II) the evidence supporting its role for cognitive processing was only correlative in nature (Canolty and Knight, 2010; Voytek et al., 2010), and (III) it remained unclear whether different coupling modes (e.g. PAC or AEC) subserve distinct cortical functions. In particular, alpha–gamma PAC has been suggested to constitute a powerful mechanism to organize visual processing (Jensen et al., 2014; Spaak et al., 2012), while theta–gamma PAC might subserve memory processes and long-range cortico-cortical communication (Axmacher et al., 2010; Canolty and Knight, 2010; Lisman and Jensen, 2013; Tort et al., 2009). Most studies focused on PAC (Canolty and Knight, 2010; Voytek et al., 2010), where gamma power is preferentially phase-locked to the trough of the theta (4–7 Hz) or the alpha (8–12 Hz) rhythm. So far, it remained elusive whether the fast or the low-frequency spectral component drives their interaction (Jiang et al., 2015; Schroeder and Lakatos, 2009; Spaak et al., 2012).

In addition, it has recently been observed that the cerebral cortex exhibits a large-scale correlation structure which is independent from phase-locked signaling and can best be analyzed by quantifying AEC (Engel et al., 2013; Hipp et al., 2012). While first applied to uncover envelope correlations within one frequency range, AEC can also be applied to the cross-frequency domain (Helfrich et al., 2014a). Fig. 1A depicts a schematic how both CFC measures (PAC and AEC) can be obtained from raw data.

*Abbreviations:* AEC, Amplitude envelope correlations; ANOVA, Analysis of variance; EEG, Electroencephalography; CFC, Cross-frequency coupling; ICM, Intrinsic coupling mode; PAC, Phase-amplitude coupling; tACS, Transcranial alternating current stimulation.

* Corresponding author at: Department of Neurophysiology and Pathophysiology, University Medical Center Hamburg-Eppendorf, 20246 Hamburg, Germany. Fax: +49 40 7410 57752.
*E-mail address:* r.helfrich@uke.de (R.F. Helfrich).

[1] These authors contributed equally to this work.

http://dx.doi.org/10.1016/j.neuroimage.2015.11.035
1053-8119/

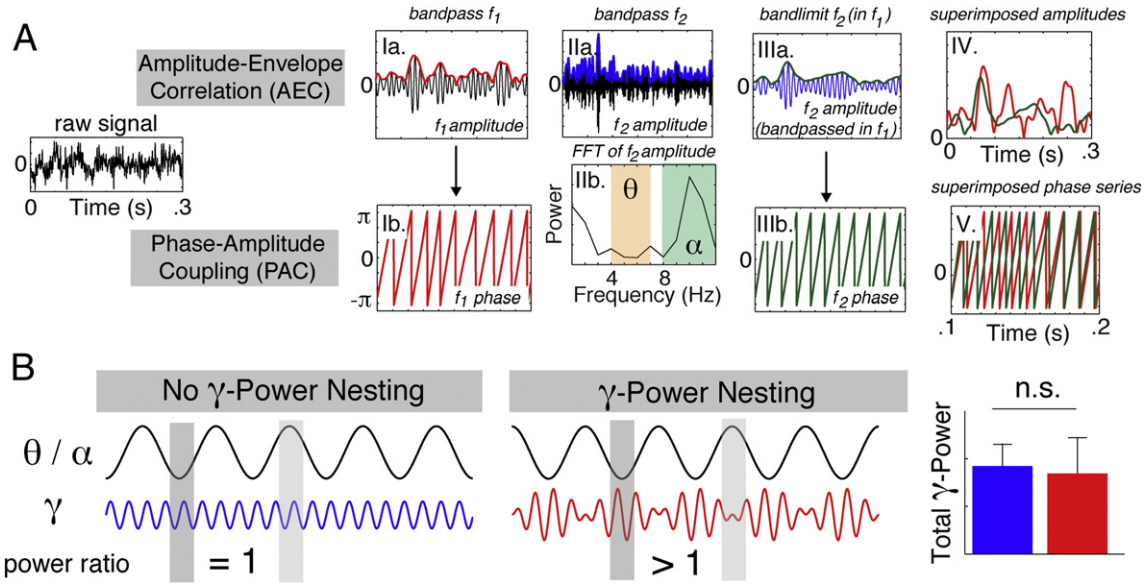


**Fig. 1.** Schematic illustration of CFC analysis. (A) Ia. Low-frequency ($f_1$) band-pass filtered signal (black) and the corresponding envelope (red) and instantaneous phase (Ib.). IIa. Gamma band-pass ($f_2$) filtered signal (black) and the corresponding envelope (blue). IIb. Fast Fourier transform (FFT) of the gamma envelope indicates that lower-frequency components modulate the instantaneous gamma amplitude. Shaded areas highlight theta (orange, 4–7 Hz) and alpha (green, 8–12 Hz) frequency ranges that were utilized for subsequent analyses. IIIa. The gamma envelope (blue, $f_2$) was filtered again in the low-frequency range ($f_1$) and then its envelope (green) and phase (IIIb.) were extracted. IV. Superposition of low-frequency amplitude (Ia.) and gamma envelope (IIIa.), which were then used for AEC analysis by means of Pearson's linear correlation coefficient (Fisher-Z-transformed). V. Superposition of low-frequency phase (Ib.) and the phase of the band-pass filtered gamma amplitude (IIIb.). Their interaction was analyzed by means of the phase-locking value (PLV; Voytek et al., 2010) to obtain the PAC. (B) Schematic of the relationship of the low-frequency (theta/alpha) and the gamma oscillation to illustrate the nesting effect, i.e. that the gamma amplitude is modulated by low-frequency fluctuations. Note that absolute power values averaged across all time points do not differ between conditions. However, in the case of nesting, gamma power becomes preferentially locked to the trough of the low-frequency oscillation, and thus, the distribution of gamma power changed on a shorter time scale (i.e. within an oscillatory cycle of the low-frequency oscillation). The power ratio was calculated as trough-locked gamma power (shaded dark gray) divided by the peak-locked gamma power (shaded light gray).

To investigate the mechanisms underlying the alpha–gamma interplay, we took advantage from a novel non-invasive brain stimulation technique, namely, transcranial alternating current stimulation (tACS; Herrmann et al., 2013; Thut et al., 2011), which has recently been demonstrated to selectively entrain neuronal oscillations within canonical frequency boundaries (Helfrich et al., 2014b; Ozen et al., 2010). Thus, this approach provided the unique opportunity to selectively drive one spectral component and study subsequent cross-frequency effects in coupled frequency bands. Here, we reanalyzed data from two combined tACS-EEG (electroencephalography) studies on visual perception, which was obtained during stimulation. Our aim was to study how cross-frequency interactions were modulated when either alpha (8–12 Hz; Helfrich et al., 2014b) or gamma (>35 Hz; Helfrich et al., 2014a) oscillations were entrained by tACS, i.e., when one of these processes was set up as the master through synchronization to the external driving force.

## Material and methods

### *Participants*

A total of 30 healthy, right-handed participants were recruited from the University of Oldenburg, Germany, and the University Medical Center Hamburg-Eppendorf, Germany. Sixteen subjects (8 female; mean age: 24.6 ± 2.8 years; 2 excluded due to technical difficulties during data acquisition) participated in study 1 and fourteen subjects (7 female; mean age: 27.5 ± 6.7 years) participated in study 2. All participants reported no history of neurological or psychiatric disease and were medication free during the experiments. They all had normal or corrected-to-normal vision and provided written informed consent according to the local ethics committee approval and the Declaration of Helsinki.

### *General procedure*

All volunteers participated in one or two sessions of the experiments carried out within 1 week. After preparation of EEG and tACS electrodes, participants completed a training session to familiarize the volunteers with the visual stimuli to ensure adequate task performance. Participants reported their percepts by button presses with their right hand. Then all participants were familiarized with skin sensations and phosphenes, which have been reported in previous tACS studies (Kanai et al., 2010; Schutter and Hortensius, 2010). However, all participants indicated that the stimulation intensity was below skin sensation and phosphene threshold. In both studies, the sham condition preceded active stimulation to avoid carry-over effects (Neuling et al., 2013).

### *Data acquisition*

#### *EEG recordings*

All experiments were conducted with participants seated comfortably in a recliner in a dimly lit, electrically shielded room to avoid line noise interference. EEG electrodes were mounted in an elastic cap (Easycap, Herrsching, Germany) prepared with a slightly abrasive electrolyte gel (Abralyt 2000, Easycap, Herrsching, Germany). EEG recordings (impedances <20 kΩ, referenced to the nose tip) were obtained using BrainAmp amplifiers (Brain Products GmbH, Gilching, Germany) from 59 electrodes in study 1 and 31 electrodes in study 2. Signals were sampled at 1000 or 5000 Hz, amplified in the range of ± 16.384 mV at a resolution of 0.5 μV and stored for offline analyses.

#### *Electrical stimulation*

In accordance with current safety limits (Nitsche et al., 2008), transcranial stimulation was applied by a battery-operated stimulator (DC-Stimulator Plus, NeuroConn, Ilmenau, Germany) via two rubber

electrodes in study 1 (Fig. 2, upper panel; 5 × 7 $cm^2$, NeuroConn, Illmenau, Germany) and via ten Ag/AgCl electrodes in study 2 (Fig. 2, lower panel; 12 mm diameter, Easycap, Herrsching, Germany; resulting in a combined electrode area of approx. 11.3 $cm^2$). Electrode placement was chosen in accordance with previous electrical brain stimulation studies targeting the extra-striate visual cortex (Neuling et al., 2013; Strüber et al., 2014). The combined impedance of all electrodes was kept below 5 kΩ, as measured by the NeuroConn tACS device, using Ten20 conductive paste (Weaver and company, Aurora, Colorado) or Signa electrolyte gel (Parker Laboratories Inc., Fairfield, NJ, USA). A sinusoidally alternating current of 1000 μA was applied at 10 or 40 Hz continuously for 20 minutes during each session. A tACS trigger was inserted every 30 cycles during the zero crossing of the external sine wave. During sham and real stimulation, the current was ramped up to 1000 μA, but discontinued after 20 seconds during the sham condition. All subjects confirmed that stimulation was acceptable and mainly noticeable during the ramp-in phase. It did not induce painful skin sensations or phosphenes. On debriefing, subjects indicated that they could not distinguish between sham and stimulation.

### *Data analysis*

Data analysis was performed using MATLAB (The MathWorks Inc., Natick, MA, USA), EEGLAB (Delorme and Makeig, 2004; http://sccn.ucsd.edu/eeglab/), FieldTrip (Oostenveld et al., 2011; http://www.ru.nl/donders/fieldtrip/), and customized MatLab Code.

All preprocessing steps were performed with EEGLab after tACS artifact removal (for details please see Helfrich et al., 2014a, 2014b). The recorded EEG was filtered using two-pass finite element response filters in the range from 1 to 100 Hz. Segments containing excessive noise, saccades, or muscle artifacts were removed after visual inspection. Data were epoched into non-overlapping three-second segments and exported to Fieldtrip for further analysis, as described previously (Helfrich et al., 2014a, 2014b). Instantaneous power and phase of different frequency bands were obtained after band-pass filtering of the data and subsequent Hilbert transformation as described below.

Cross-frequency interactions between the slow oscillation (theta: 4–7 Hz; alpha: 8–12 Hz) and gamma (46–70 Hz) were assessed for every channel, condition, and subject separately. The gamma range was chosen in accordance with a recent report to keep results comparable (Helfrich et al., 2014a). In order to calculate the amplitude-envelope correlation between both, we first band-pass filtered every data segment of interest in the low-frequency range and in the gamma range, similar to the approach, which had been introduced and validated before (Voytek et al., 2010).

### *Amplitude-envelope correlations*

We utilized a two-way, zero phase-lag, finite impulse response (FIR) filter (eegfilt.m function in EEGLab toolbox; Delorme and Makeig, 2004) to prevent phase distortion. Hilbert's transform was applied to the band-pass filtered low-frequency signal to extract its amplitude and the instantaneous phase. Then a second Hilbert transform was utilized to extract the amplitude of the gamma oscillation, which was band-pass filtered in the low-frequency range. Subsequently, a third Hilbert transform was used to extract the envelope and the instantaneous phase of the low-frequency band-pass filtered gamma amplitude. Amplitude-envelope correlations (AEC) between the low-frequency amplitude and the gamma envelope in the respective frequency range were calculated for every trial separately. Subsequently, Pearson's linear correlation values were Fisher-Z-transformed and averaged across trials.

### *Phase-amplitude coupling*

Phase-amplitude coupling (PAC) was calculated by means of the phase-locking technique (Lachaux et al., 1999; Voytek et al., 2010) between the instantaneous phase of the low-frequency oscillation and the instantaneous phase of the gamma amplitude after band-pass filtering in the low-frequency range. Fig. 1A provides a brief overview of how both measures were obtained.

### *Nested power analyses*

To calculate the gamma power relative to the low-frequency oscillation, the analytic amplitude of the gamma-filtered signal was grouped into four equally sized phase-bins, given the design of one of the studies (Helfrich et al., 2014b), relative to the phase of the low-frequency oscillation (centered on the trough, the peak, and the two zero-crossings). Then the amplitude values were squared to obtain the oscillatory power. In order to determine the amount of nesting of the gamma power relative to the low oscillatory phase, a power ratio (PR) was calculated as gamma power (locked to the trough of the slow-frequency component) divided by the gamma power (locked to the peak of the slow-frequency component). In case of no nesting of gamma power, the value is 1, i.e. the gamma power does not differ between peak and trough. Values >1 indicate increased nesting, i.e. higher gamma power

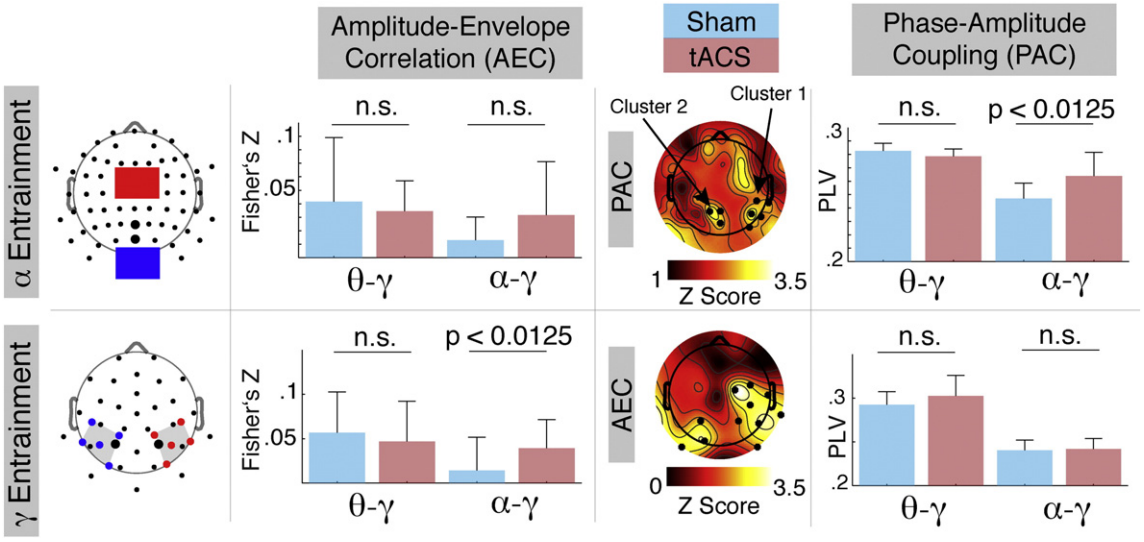


**Fig. 2.** Intrinsic coupling modes of cross-frequency interactions. Upper row: The electrode montage of study 1 (Helfrich et al., 2014b); electrodes-of-interest are bold; red and blue electrodes depict tACS electrodes), AEC and PAC (mean ± STD) results along with the topography highlighting two significant clusters (black dots) of increased alpha–gamma PAC during 10 Hz tACS. Lower row: Electrode montage, AEC and PAC results from study 2 (Helfrich et al., 2014a). The topography depicts the increased alpha–gamma AEC during 40 Hz tACS.

during the trough than during the peak of low-frequency oscillation, while values <1 point to the opposite. Fig. 1B illustrates the nesting effect. Please note that the PAC and the power ratio are highly related measures. Here, we analyzed both measures (a) to quantify the impact of changes in PAC, (b) to provide a mechanistic understanding of the function of PAC, and (c) to provide a second measure to quantify the phase-locking technique (Voytek et al., 2010).

*Statistical analyses*

We utilized analyses of variance (ANOVA) with Bonferroni-corrected t-tests according to the initial hypotheses at the channels-of-interest. Therefore, PAC and AEC analyses were corrected for 4 comparisons ($p = 0.05/4 = 0.0125$), while the power nesting analyses were corrected for 2 comparisons ($p = 0.05/2 = 0.025$). Effect sizes were quantified by means of Cohen's d (Cohen, 1988), where values >0.8 highlight a strong effect, values <0.4 indicate no effect. Intermediate values signal a moderate effect size. All values reported are mean ± standard deviation unless stated otherwise. The regional specificity of the observed effects was confirmed with cluster-based permutation statistics as implemented in Fieldtrip (Monte Carlo method). The cluster approach corrects for the multiple comparison problem (Maris and Oostenveld, 2007). Dependent-samples t-tests were computed at each sensor and for each cross-frequency interaction. Clusters were obtained by summing up t-values, which were adjacent in space and frequency below a cluster alpha level of 5%. A permutation distribution was computed by randomly switching condition labels within subjects in each of 1000 iterations. The permutation p-value was obtained by comparing the cluster statistic to the random permutation distribution. The observed clusters were considered independently significant when the sum of t-values exceeded 95% of the permutated distribution.

## Results

In a previous study, we found that alpha power was increased during 10 Hz tACS as compared to sham (Helfrich et al., 2014b; +49.3% ± 21.8% (mean ± SEM); $t_{13} = -2.26$, $p = 0.04$). Entrainment was quantified by means of circular statistics, revealing a non-uniform phase distribution in presence of the externally applied electric field, as well as by increments in inter-trial coherence and phase-locking to the externally applied sine wave (for details and statistics, please see Fig. 4 in Helfrich et al., 2014b). In addition, we also recently reported that 40 Hz tACS selectively entrains gamma oscillations, as quantified by non-uniform gamma phase distributions during tACS as well as reduced network entropy (for details and statistics, please see Fig. 6 in Helfrich et al., 2014a). Interestingly, the results from the latter study indicated that gamma entrainment did not modulate gamma power ($t_{13} = 1.23$, $p = 0.24$; see also below in Section 3.2). However, alpha power was reduced in response to gamma entrainment as compared to sham (−21.0% ± 6.7% (mean ± SEM); $t_{13} = 3.13$, $p = 0.008$), indicating a co-modulation of nested or coupled neuronal networks across several temporal scales (Canolty and Knight, 2010; Jensen et al., 2014).

*Modulation of cross-frequency interactions by tACS*

In order to assess the impact of selective entrainment of one frequency band on nested or coupled neuronal networks, we assessed cross-frequency interactions by means of two established coupling measures, namely, PAC and AEC, which have previously been related to different cortical functions (Engel et al., 2013). Here, we investigated how theta–gamma and alpha–gamma interactions were modulated during the selective entrainment of either alpha or gamma oscillations. We assessed the influence of the *entrainment frequency* (10 or 40 Hz) on both *coupling modes* (PAC and AEC) for two *cross-frequency interactions* (theta–gamma and alpha–gamma) by means of a mixed ANOVA. We found a significant effect of *cross-frequency interactions* ($F_{1,13} = 6.95$, $p = 0.02$) as well as a significant interaction of *coupling mode x cross-frequency interaction* ($F_{1,13} = 5.60$, $p = 0.03$). Importantly, we found a 3-way interaction ($F_{1,13} = 4.96$, $p = 0.04$), while all other factors and interactions remained non-significant (*coupling modes*: $F_{1,13} = 0.006$, $p = 0.94$; *entrainment frequency × coupling mode*: $F_{1,13} = 0.05$, $p = 0.83$; *entrainment frequency × cross-frequency interaction*: $F_{1,13} = 0.50$, $p = 0.49$). In order to resolve the 3-way interaction, we analyzed both studies separately by means of post hoc Bonferroni-corrected t-tests.

Our results indicate that only alpha–gamma PAC was increased during alpha entrainment ($t_{13} = 3.77$, $p = 0.002$, $d = 1.13$; Fig. 2), while neither theta–gamma PAC ($t_{13} = -1.74$, $p = 0.11$; $d = -0.71$) nor AECs (theta–gamma: $t_{13} = -0.66$, $p = 0.52$, $d = 0.04$; alpha–gamma: $t_{13} = 1.46$, $p = 0.17$, $d = 0.61$) differed significantly between sham and stimulation. This effect was confined to two parieto-occipital clusters (cluster 1: $p = 0.003$; cluster 2: $p = 0.005$; Fig. 2). The results demonstrated a regional-specific increase in alpha–gamma PAC during alpha entrainment.

During gamma-band entrainment, we observed an increase in alpha–gamma AEC ($t_{13} = 3.82$, $p = 0.002$, $d = 0.71$). This effect was regionally specific (cluster test: $p = 0.005$) and confined to the stimulated parieto-occipital cortex. In addition, this effect was also frequency-specific (theta–gamma AEC: $t_{13} = -0.73$, $p = 0.47$, $d = -0.22$) and was not accompanied by changes in PAC (theta–gamma: $t_{13} = 1.30$, $p = 0.22$, $d = 0.50$; alpha–gamma: $t_{13} = 0.44$, $p = 0.67$, $d = 0.12$). Interestingly, the strength of the alpha–gamma AEC modulation over parieto-occipital cortex (tACS–sham) closely correlated with the individual alpha power suppression during stimulation (Pearson linear correlation: $r = 0.66$, $p = 0.01$), indicating that increased alpha–gamma AEC led to stronger alpha power suppression.

*Differential modulation of power nesting by tACS*

To quantify the impact on gamma power during alpha band entrainment, we first analyzed power differences between sham and stimulation and did not observe a significant difference ($t_{13} = -0.15$, $p = 0.88$, $d = -0.06$; Fig. 3A). Secondly, we assessed whether the distribution of gamma power relative to low-frequency phase was modulated, i.e. whether gamma power was now preferentially locked to the trough of the low-frequency phase (so called nesting; for an illustration see Fig. 1B). Hence, we analyzed a power ratio, where alpha-trough-locked gamma power was divided by alpha-peak-locked gamma power and found a significant cluster in parieto-occipital cortex ($p = 0.02$; $d = 0.73$; Fig. 3B), corresponding to cluster 1 of increased PAC during stimulation (Fig. 2). This finding was consistent with an increased nesting of gamma power. We only found one significant cluster, most likely due to the small size of cluster 2, which consisted only of 3 electrodes (Fig. 2). This result indicates a frequency-specific locking of gamma power to the trough of the alpha oscillation, since the gamma-power ratio was not modulated relative to the theta-phase (cluster test: $p > 0.05$, $d = -0.26$; Fig. 3B).

Previously, we reported that gamma oscillations were selectively entrained by 40 Hz tACS without concomitant gamma power changes ($t_{13} = 1.23$, $p = 0.24$, $d = 0.47$; Fig. 3C; Helfrich et al., 2014a). Here, we assessed whether changes in AEC were accompanied by changes in gamma power relative to the phase of the low oscillations, but found no evidence for this (Fig. 3D; cluster test: all $p > 0.05$; theta–gamma: $d = 0.37$, alpha–gamma: $d = -0.04$).

## Discussion

Our results demonstrate that selective driving of alpha or gamma oscillations differentially modulated their physiological interaction. Entrainment of alpha oscillations increased PAC and promoted a preferential phase-locking of gamma power to the alpha trough, while gamma-band entrainment modulated AECs. These results indicate that both can serve as master and slave through distinct coupling modes, possibly

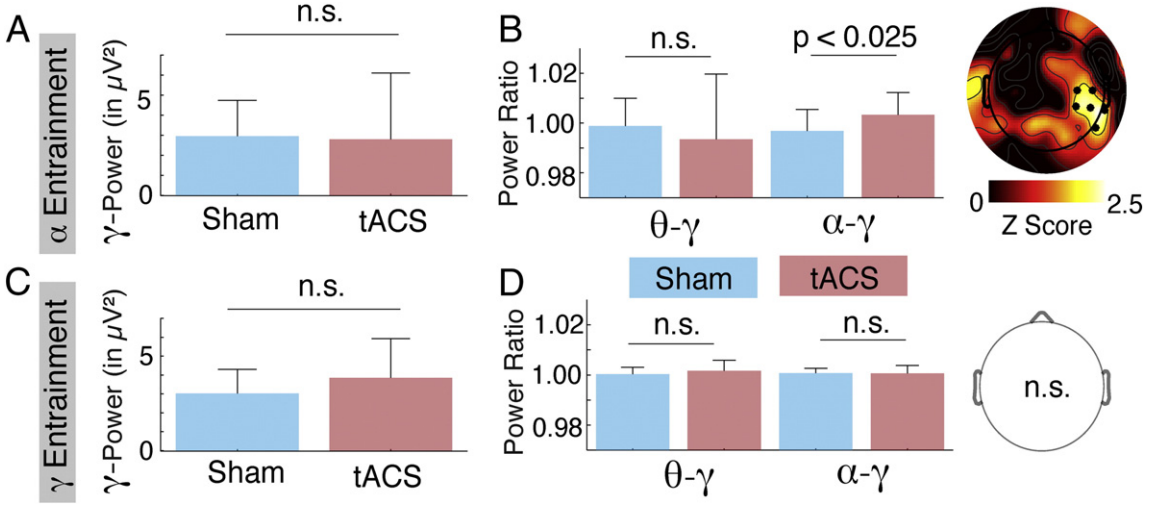


**Fig. 3.** Spectral power and nesting results. (A) The grand-average gamma power results from study 1 (Helfrich et al., 2014b; electrodes of interest) indicate that there was no significant gamma power difference between sham and stimulation. (B) One significant cluster of increased gamma power nesting in the alpha phase during 10 Hz tACS in study 1 was found over lateral parieto-occipital sensors, corresponding to cluster 1 of increased PAC during stimulation (Fig. 2). (C) Grand-average gamma power results from study 2 (Helfrich et al., 2014a; electrodes of interest) indicate that gamma power did not differ between sham and stimulation. (D) No gamma power nesting effects were observed during 40 Hz tACS.

working as opponent processes to subserve different cortical functions (Schroeder and Lakatos, 2009).

*Intrinsic coupling modes and alpha–gamma CFC*

Phase or amplitude coupling are regularly observed in electrophysiological data and have recently been conceptualized as different types of intrinsic coupling modes (ICMs, Engel et al., 2013), which possibly subserve different cortical computations. While amplitude coupling might regulate the activation of distributed neuronal populations, phase coupling is thought to mediate specific inter-areal cortical information flow (Engel et al., 2013; Fries, 2005; Hipp et al., 2012). Recently, it has been demonstrated that inter-areal feedforward and feedback mechanisms in visual areas might be implemented on different temporal scales (Bastos et al., 2014), leaving the question unaddressed how different temporal scales exert their feedback and feedforward influences (Jensen et al., 2015). While previous evidence indicated that low-frequency oscillations might drive cortical gamma rhythms (Canolty and Knight, 2010; Schroeder and Lakatos, 2009; Spaak et al., 2012), a recent simulation and electrocorticography study suggested that the gamma envelope drives cortical alpha oscillations (Jiang et al., 2015). Our present results indicate that both spectral components might be dynamically established as master or slave through different coupling modes. Therefore, different coupling modes might serve as a mechanism to mediate cortical communication across temporal scales.

The present results extend the concept of ICMs beyond their role for inter-areal communication and suggest that interactions between both coupling modes might constitute a feedback mechanism that balances the relation between slow and fast oscillatory rhythms within and across cortical areas. Thus, different coupling modes might subserve the optimization of cortical processing dynamics and increase cortical coding capacity.

These results are in line with previous correlative evidence, which suggested that coupled alpha and gamma oscillations constitute the functional architecture of the visual system and subserve sensory input selection, attentional control, and short-term visual memory (Jensen et al., 2014; Spaak et al., 2012). Hence, the present results provide causal evidence for the physiological antagonistic alpha–gamma interplay (Jensen et al., 2014; Osipova et al., 2008; Voytek et al., 2010), given that all effects were limited to their interaction in the stimulated parieto-occipital cortex during visual tasks.

The differential response of oscillatory alpha activity to 10 or 40 Hz tACS now allows a selective up-regulation by alpha-tACS (entrainment; Helfrich et al., 2014b; Herrmann et al., 2013) or the selective down-regulation of alpha activity by gamma-tACS (enslavement; Boyle and Fröhlich, 2013; Helfrich et al., 2014a). In future studies, this approach may allow a more refined characterization of the role of alpha oscillations for visual perception and extend previous correlative evidence (Jensen et al., 2014).

*Physiological efficacy of tACS*

So far, tACS has been suggested to operate in canonical frequency boundaries via directed entrainment of ongoing oscillatory activity (Herrmann et al., 2013). Importantly, entrainment is characterized by a set of criteria (Thut et al., 2011): (I) A periodic driving force in the input stream needs to interact with (II) a neuronal oscillator (III) through synchronization by (IV) direct interaction. Here, we only observed a power increment during alpha- (Helfrich et al., 2014b) but not during gamma-band entrainment (Helfrich et al., 2014a). These findings are in line with previous studies (Neuling et al., 2013; Strüber et al., 2014) and support the idea that weak entrainment affects the phase of the ongoing activity, while stronger entrainment modulates phase and power (Herrmann et al., 2013; Neuling et al., 2013). Thus, power increments are not essential to entrainment.

The present results extend previous findings that tACS modulates neuronal activity across spatial scales (Polanía et al., 2012; Strüber et al., 2014) toward the idea that tACS also modulates neuronal activity across several temporal scales. This is in line with several other recent studies, which also suggested that secondary effects might occur across different temporal scales in coupled or nested neuronal networks (Boyle and Fröhlich, 2013; Neuling et al., 2012; Wach et al., 2013). Thus, cross-frequency effects and co-modulations of coupled networks might explain previous equivocal findings in tACS studies (Brignani et al., 2013).

*Confounds and limitations*

It is the nature of non-invasive brain stimulation that its effects are often small (Thut et al., 2011). In particular, since it has been demonstrated that effects are cortical (Neuling et al., 2013) and cognitive state dependent (Bestmann et al., 2015). Here, we observed a differential modulation of CFC through different driving frequencies. The effects

on gamma power distributions relative to the phase of the ongoing low-frequency oscillation were significant and physiologically plausible, even though absolute changes were small (Fig. 3B). Several limitations apply to the present results given the design of the initial studies with (I) different strategies to suppress the tACS artifact, (II) different visual tasks and procedures, (III) different EEG and stimulation electrode placements, and therefore (IV) different electrodes-of-interest, as well as (V) the a priori defined frequency bands or phase angles of interest. However, both stimulation protocols (Helfrich et al., 2014a, 2014b) targeted the extra-striate visual cortex while participants were engaged in visual tasks. Importantly, all observed effects were confined to the stimulated parieto-occipital cortex and the physiological alpha–gamma interaction. These findings make it less likely that the observed effects were related to residual stimulation artifacts or the electrical activation of cranial muscles. To date, only a few methods have been utilized to suppress the tACS artifact in electrophysiological recordings (Helfrich et al., 2014a, 2014b; Neuling et al., 2015; Voss et al., 2014) and more refined approaches in the future will hopefully provide more detailed insights into the physiological efficacy of tACS.

Furthermore, the choice of the reference electrode could have an impact on the posterior gamma power and CFC estimates (Yuval-Greenberg et al., 2008). However, it is unlikely that this effect varies as a function of the low-frequency or the coupling mode. In order to rule out this possibility, we repeated all analyses based on common average referenced data and obtained highly similar results.

The present studies provide the first evidence that tACS modulates oscillatory brain activity across several temporal scales within physiological boundaries. The present results might extend our understanding of the mechanisms which orchestrate cross-frequency coupling (Engel et al., 2013; Schroeder and Lakatos, 2009). We assume that spatially and temporally targeted stimulation approaches, which aim to modulate task-related CFC (Voytek et al., 2010) will yield a better understanding and enhanced efficacy of tACS in the future.

### *Conclusions*

The present results extend previous correlative studies by a causal dimension. Here, we established phase–power as well as power–power couplings as important mechanisms of cortical processing and specific multi-site communication in coupled oscillatory networks. The present results indicate that tACS can be used as a powerful tool to assess the causal role of CFC for cortical computations, which seems helpful given the various pitfalls that hamper the correlative analysis of CFC (Aru et al., 2014). In addition, they provide the first evidence that tACS effects have to be interpreted as network effects, possibly spanning several spatiotemporal scales. Taken together, this approach provides a novel opportunity to study the role of CFC for normal and impaired brain function (Fröhlich and Schmidt, 2013). Therefore, our results have strong implications for future research on neuropsychiatric diseases, such as schizophrenia or Parkinson's disease, which all have been related to impaired neuronal synchronization or cross-frequency processes (Schulz et al., 2013).

## Acknowledgements

The authors declare no competing financial interests. This work was supported by grants from the European Union (ERC-2010-AdG-269716, AKE), the German Research Foundation (SFB936/A3/Z1, AKE; SFB/TRR 31, CSH; SPP1665 EN 533/13-1, AKE; SPP1665 HE 3353/8-1, CSH), the German National Academic Foundation (RFH) and the Alexander von Humboldt Foundation (Feodor Lynen Program, RFH).

## References

Aru, J., Aru, J., Priesemann, V., Wibral, M., Lana, L., Pipa, G., Singer, W., Vicente, R., 2014. Untangling cross-frequency coupling in neuroscience. Curr. Opin. Neurobiol. 31C, 51–61. http://dx.doi.org/10.1016/j.conb.2014.08.002.

Axmacher, N., Henseler, M.M., Jensen, O., Weinreich, I., Elger, C.E., Fell, J., 2010. Cross-frequency coupling supports multi-item working memory in the human hippocampus. Proc. Natl. Acad. Sci. 107, 3228–3233. http://dx.doi.org/10.1073/pnas.0911531107.

Bastos, A.M., Vezoli, J., Bosman, C.A., Schoffelen, J.-M., Oostenveld, R., Dowdall, J.R., De Weerd, P., Kennedy, H., Fries, P., 2014. Visual areas exert feedforward and feedback influences through distinct frequency channels. Neuron http://dx.doi.org/10.1016/j.neuron.2014.12.018.

Bestmann, S., de Berker, A.O., Bonaiuto, J., 2015. Understanding the behavioural consequences of noninvasive brain stimulation. Trends Cogn. Sci. 19, 13–20. http://dx.doi.org/10.1016/j.tics.2014.10.003.

Boyle, M.R., Fröhlich, F., 2013. EEG feedback-controlled transcranial alternating current stimulation. 2013 6th International IEEE/EMBS Conference on Neural Engineering (NER). Presented at the 2013 6th International IEEE/EMBS Conference on Neural Engineering (NER), pp. 140–143 http://dx.doi.org/10.1109/NER.2013.6695891.

Brignani, D., Ruzzoli, M., Mauri, P., Miniussi, C., 2013. Is transcranial alternating current stimulation effective in modulating brain oscillations? PLoS One 8, e56589. http://dx.doi.org/10.1371/journal.pone.0056589.

Canolty, R.T., Knight, R.T., 2010. The functional role of cross-frequency coupling. Trends Cogn. Sci. 14, 506–515. http://dx.doi.org/10.1016/j.tics.2010.09.001.

Cohen, J., 1988. Statistical Power Analysis for the Behavioral Sciences. L. Erlbaum Associates.

Delorme, A., Makeig, S., 2004. EEGLAB: an open source toolbox for analysis of single-trial EEG dynamics including independent component analysis. J. Neurosci. Methods 134, 9–21. http://dx.doi.org/10.1016/j.jneumeth.2003.10.009.

Engel, A.K., Gerloff, C., Hilgetag, C.C., Nolte, G., 2013. Intrinsic coupling modes: multiscale interactions in ongoing brain activity. Neuron 80, 867–886. http://dx.doi.org/10.1016/j.neuron.2013.09.038.

Fries, P., 2005. A mechanism for cognitive dynamics: neuronal communication through neuronal coherence. Trends Cogn. Sci. 9, 474–480. http://dx.doi.org/10.1016/j.tics.2005.08.011.

Fröhlich, F., Schmidt, S.L., 2013. Rational design of transcranial current stimulation (TCS) through mechanistic insights into cortical network dynamics. Front. Hum. Neurosci. 7, 804. http://dx.doi.org/10.3389/fnhum.2013.00804.

Helfrich, R.F., Knepper, H., Nolte, G., Strüber, D., Rach, S., Herrmann, C.S., Schneider, T.R., Engel, A.K., 2014a. Selective modulation of interhemispheric functional connectivity by HD-tACS shapes perception. PLoS Biol. 12, e1002031. http://dx.doi.org/10.1371/journal.pbio.1002031.

Helfrich, R.F., Schneider, T.R., Rach, S., Trautmann-Lengsfeld, S.A., Engel, A.K., Herrmann, C.S., 2014b. Entrainment of brain oscillations by transcranial alternating current stimulation. Curr. Biol. 24, 333–339. http://dx.doi.org/10.1016/j.cub.2013.12.041.

Herrmann, C.S., Rach, S., Neuling, T., Strüber, D., 2013. Transcranial alternating current stimulation: a review of the underlying mechanisms and modulation of cognitive processes. Front. Hum. Neurosci. 279. http://dx.doi.org/10.3389/fnhum.2013.00279.

Hipp, J.F., Hawellek, D.J., Corbetta, M., Siegel, M., Engel, A.K., 2012. Large-scale cortical correlation structure of spontaneous oscillatory activity. Nat. Neurosci. 15, 884–890. http://dx.doi.org/10.1038/nn.3101.

Jensen, O., Bonnefond, M., Marshall, T.R., Tiesinga, P., 2015. Oscillatory mechanisms of feedforward and feedback visual processing. Trends Neurosci. 38, 192–194. http://dx.doi.org/10.1016/j.tins.2015.02.006.

Jensen, O., Gips, B., Bergmann, T.O., Bonnefond, M., 2014. Temporal coding organized by coupled alpha and gamma oscillations prioritize visual processing. Trends Neurosci. 37, 357–369. http://dx.doi.org/10.1016/j.tins.2014.04.001.

Jiang, H., Bahramisharif, A., van Gerven, M.A.J., Jensen, O., 2015. Measuring directionality between neuronal oscillations of different frequencies. NeuroImage 118, 359–367. http://dx.doi.org/10.1016/j.neuroimage.2015.05.044.

Kanai, R., Paulus, W., Walsh, V., 2010. Transcranial alternating current stimulation (tACS) modulates cortical excitability as assessed by TMS-induced phosphene thresholds. Clin. Neurophysiol. Off. J. Int. Fed. Clin. Neurophysiol. 121, 1551–1554. http://dx.doi.org/10.1016/j.clinph.2010.03.022.

Lachaux, J.P., Rodriguez, E., Martinerie, J., Varela, F.J., 1999. Measuring phase synchrony in brain signals. Hum. Brain Mapp. 8, 194–208.

Lisman, J.E., Jensen, O., 2013. The θ-γ neural code. Neuron 77, 1002–1016. http://dx.doi.org/10.1016/j.neuron.2013.03.007.

Maris, E., Oostenveld, R., 2007. Nonparametric statistical testing of EEG- and MEG-data. J. Neurosci. Methods 164, 177–190. http://dx.doi.org/10.1016/j.jneumeth.2007.03.024.

Neuling, T., Rach, S., Herrmann, C.S., 2013. Orchestrating neuronal networks: sustained after-effects of transcranial alternating current stimulation depend upon brain states. Front. Hum. Neurosci. 7, 161. http://dx.doi.org/10.3389/fnhum.2013.00161.

Neuling, T., Rach, S., Wagner, S., Wolters, C.H., Herrmann, C.S., 2012. Good vibrations: oscillatory phase shapes perception. NeuroImage 63, 771–778. http://dx.doi.org/10.1016/j.neuroimage.2012.07.024.

Neuling, T., Ruhnau, P., Fuscà, M., Demarchi, G., Herrmann, C.S., Weisz, N., 2015. Friends, not foes: magnetoencephalography as a tool to uncover brain dynamics during transcranial alternating current stimulation. NeuroImage 118, 406–413. http://dx.doi.org/10.1016/j.neuroimage.2015.06.026.

Nitsche, M.A., Cohen, L.G., Wassermann, E.M., Priori, A., Lang, N., Antal, A., Paulus, W., Hummel, F., Boggio, P.S., Fregni, F., Pascual-Leone, A., 2008. Transcranial direct current stimulation: state of the art 2008. Brain Stimul. 1, 206–223. http://dx.doi.org/10.1016/j.brs.2008.06.004.

Oostenveld, R., Fries, P., Maris, E., Schoffelen, J.-M., 2011. FieldTrip: open source software for advanced analysis of MEG, EEG, and invasive electrophysiological data. Comput. Intell. Neurosci. 2011, 156869. http://dx.doi.org/10.1155/2011/156869.

Osipova, D., Hermes, D., Jensen, O., 2008. Gamma power is phase-locked to posterior alpha activity. PLoS One 3, e3990. http://dx.doi.org/10.1371/journal.pone.0003990.
Ozen, S., Sirota, A., Belluscio, M.A., Anastassiou, C.A., Stark, E., Koch, C., Buzsáki, G., 2010. Transcranial electric stimulation entrains cortical neuronal populations in rats. J. Neurosci. Off. J. Soc. Neurosci. 30, 11476–11485. http://dx.doi.org/10.1523/JNEUROSCI.5252-09.2010.
Polanía, R., Nitsche, M.A., Korman, C., Batsikadze, G., Paulus, W., 2012. The importance of timing in segregated theta phase-coupling for cognitive performance. Curr. Biol. 22, 1314–1318. http://dx.doi.org/10.1016/j.cub.2012.05.021.
Schroeder, C.E., Lakatos, P., 2009. The gamma oscillation: master or slave? Brain Topogr. 22, 24–26. http://dx.doi.org/10.1007/s10548-009-0080-y.
Schulz, R., Gerloff, C., Hummel, F.C., 2013. Non-invasive brain stimulation in neurological diseases. Neuropharmacology 64, 579–587. http://dx.doi.org/10.1016/j.neuropharm.2012.05.016.
Schutter, D.J.L.G., Hortensius, R., 2010. Retinal origin of phosphenes to transcranial alternating current stimulation. Clin. Neurophysiol. Off. J. Int. Fed. Clin. Neurophysiol. 121, 1080–1084. http://dx.doi.org/10.1016/j.clinph.2009.10.038.
Siegel, M., Donner, T.H., Engel, A.K., 2012. Spectral fingerprints of large-scale neuronal interactions. Nat. Rev. Neurosci. 13, 121–134. http://dx.doi.org/10.1038/nrn3137.
Spaak, E., Bonnefond, M., Maier, A., Leopold, D.A., Jensen, O., 2012. Layer-specific entrainment of γ-band neural activity by the α rhythm in monkey visual cortex. Curr. Biol. 22, 2313–2318. http://dx.doi.org/10.1016/j.cub.2012.10.020.
Strüber, D., Rach, S., Trautmann-Lengsfeld, S.A., Engel, A.K., Herrmann, C.S., 2014. Antiphasic 40 Hz oscillatory current stimulation affects bistable motion perception. Brain Topogr. 27, 158–171. http://dx.doi.org/10.1007/s10548-013-0294-x.
Thut, G., Schyns, P.G., Gross, J., 2011. Entrainment of perceptually relevant brain oscillations by non-invasive rhythmic stimulation of the human brain. Front. Psychol. 2, 170. http://dx.doi.org/10.3389/fpsyg.2011.00170.
Tort, A.B.L., Komorowski, R.W., Manns, J.R., Kopell, N.J., Eichenbaum, H., 2009. Theta–gamma coupling increases during the learning of item–context associations. Proc. Natl. Acad. Sci. 106, 20942–20947. http://dx.doi.org/10.1073/pnas.0911331106.
Voss, U., Holzmann, R., Hobson, A., Paulus, W., Koppehele-Gossel, J., Klimke, A., Nitsche, M.A., 2014. Induction of self awareness in dreams through frontal low current stimulation of gamma activity. Nat. Neurosci. 17, 810–812. http://dx.doi.org/10.1038/nn.3719.
Voytek, B., Canolty, R.T., Shestyuk, A., Crone, N.E., Parvizi, J., Knight, R.T., 2010. Shifts in gamma phase-amplitude coupling frequency from theta to alpha over posterior cortex during visual tasks. Front. Hum. Neurosci. 4, 191. http://dx.doi.org/10.3389/fnhum.2010.00191.
Wach, C., Krause, V., Moliadze, V., Paulus, W., Schnitzler, A., Pollok, B., 2013. The effect of 10 Hz transcranial alternating current stimulation (tACS) on corticomuscular coherence. Front. Hum. Neurosci. 7, 511. http://dx.doi.org/10.3389/fnhum.2013.00511.
Yuval-Greenberg, S., Tomer, O., Keren, A.S., Nelken, I., Deouell, L.Y., 2008. Transient induced gamma-band response in EEG as a manifestation of miniature saccades. Neuron 58, 429–441. http://dx.doi.org/10.1016/j.neuron.2008.03.027.